Structure and Bonding of the Isoelectronic Hexacarbonyls $[Hf(CO)_6]^{2-}$, $[Ta(CO)_6]^{-}$, $W(CO)_6$, $[Re(CO)_6]^{+}$, $[Os(CO)_6]^{2+}$, and $[Ir(CO)_6]^{3+}$: A Theoretical Study[1]

Robert K. Szilagyi[†] and Gernot Frenking*

Fachbereich Chemie, Philipps-Universität Marburg, Hans-Meerwein-Strasse, D-35032 Marburg, Germany

Received August 4, 1997[⊗]

Equilibrium geometries, vibrational frequencies, and metal−CO bond dissociation energies of the title compounds have been calculated using quantum-chemical methods at the DFT (B3LYP and BP86) and CCSD(T)//MP2 levels of theory, utilizing relativistic effective core potentials for the metals. The nature of the metal−CO interactions has been analyzed using the CDA method. The theoretically predicted geometries and vibrational spectra at B3LYP, BP86, and MP2 are in good agreement with experimental data. The calculated C−O bond lengths show a regular decrease and the C−O stretching frequencies increase from $[Hf(CO)_6]^{2-}$ to $[Ir(CO)_6]^{3+}$. The calculated first dissociation energies (FDE) of one CO show the trend $[Ir(CO)_6]^{3+} > [Os(CO)_6]^{2+} > [Hf(CO)_6]^{2-} > [Re(CO)_6]^{+} > W(CO)_6 \approx [Ta(CO)_6]^{-}$, which does not correlate with the C−O bond length. A remarkable result of the calculations is that the highest FDE is predicted for $[Ir(CO)_6]^{3+}$, which has very little IR→CO π-back-donation. The high FDEs of $[Ir(CO)_6]^{3+}$ and $[Os(CO)_6]^{2+}$ are explained by the strong OC→metal σ-donation, which leads to a large charge transfer from the six CO ligands to the metal. B3LYP and BP86 give bond energies similar to those of CCSD(T) at MP2-optimized geometries. The CDA method shows a regular decrease of metal→CO π-back-donation from $[Hf(CO)_6]^{2-}$ to $[Ir(CO)_6]^{3+}$. Optimization of the C−O bond length as a function of the Hf−CO distance of $[Hf(CO)_6]^{2-}$ gives a smooth curve from the equilibrium value, which is longer than in free CO, to the value of free CO. The corresponding curves for single CO dissociation from $W(CO)_6$ and $Cr(CO)_6$ have a turning point where the C−O distance is shorter than in free CO. The C−O bond of $[Ir(CO)_6]^{3+}$, which is shorter than in free CO, becomes even slightly shorter when the Ir−CO distance is stretched by up to ∼0.25 Å, before it becomes longer and approaches the value of free CO. The CDA results show that the change in the C−O bond length can be explained by the M→CO π-back-donation and M↔CO repulsive polarization. The repulsive polarization seems to be more important than the π-back-donation for $Ir(CO)_6^{3+}$. The model of metal−CO interactions which is used by Strauss to distinguish between classical and nonclassical carbonyls is supported by the present study.

Introduction

The understanding of transition-metal−ligand bonding has become much deeper in the last couple of years, because modern methods of theoretical chemistry have made it possible to calculate transition-metal complexes with high accuracy.[2] The theoretically predicted geometries and bond energies are in very good agreement with experimental data, which are much more difficult to obtain reliably than theoretical results. This was made feasible by the great progress in the development of density functional theory (DFT)[3] and the use of effective core potentials (ECP)[4] in quantum-mechanical calculations.[2] The analysis of the calculated results gives new insights into the nature of metal−ligand interactions, which can be used to examine the validity of qualitatively derived models of chemical bonding. Either this leads to support and a subsequent refinement of the existing model or it may be shown that apparently plausible assumptions are not justified. For example, Davidson[5] has recently shown that, in transition-metal carbonyl complexes, metal→CO π-back-donation is more important for the binding energy than OC→M σ-donation, although the overlap and the charge

[†] Permanent address: Müller Laboratory, Department of Organic Chemistry, University of Veszprem, P.O. Box 158, H 8201 Veszprem, Hungary.

[⊗] Abstract published in *Advance ACS Abstracts,* September 15, 1997.

(1) Theoretical Studies of Organometallic Compounds. 26. Part 25: Fröhlich, N.; Pidun, U.; Stahl, M.; Frenking, G. *Organometallics* **1997**, *16*, 442.

(2) Reviews: (a) Frenking, G.; Antes, I.; Böhme, M.; Dapprich, S.; Ehlers, A. W.; Jonas, V.; Neuhaus, A.; Otto, M.; Stegmann, R.; Veldkamp, A.; Vyboishchikov, S. F. In *Reviews in Computational Chemistry*; Lipkowitz, K. B., Boyd, D. B. Eds.; VCH: New York, 1996; Vol. 8, pp 63−144. (b) Cundari, T. R.; Benson, M. T.; Lutz, M. L.; Sommerer, S. O. In *Reviews in Computational Chemistry*; Lipkowitz, K. B., Boyd, D. B., Eds.; VCH: New York, 1996; Vol. 8, pp 145−202. (c) Ziegler, T. *Chem. Rev.* **1991**, *91*, 651.

(3) Nalewajski, R. F., Ed. *Density Functional Theory I−IV*; Topics in Current Chemistry 180−183; Springer-Verlag: Heidelberg, Germany, 1996.

(4) Szasz, L. *Pseudopotential Theory of Atoms and Molecules*; Wiley: New York, 1986. Krauss, M.; Stevens, W. J. *Annu. Rev. Phys. Chem.* **1984**, *35*, 357.

(5) Davidson, E. R.; Kunze, K. L.; Machado, F. B. C.; Chakravorty, S. J. *Acc. Chem. Res.* **1993**, *26*, 628 and further references cited in this work.

S0276-7333(97)00671-7 CCC: $14.00

donation of the σ orbitals are higher than those of the π orbitals.[6] The Dewar−Chatt−Duncanson model[7] of synergistic ligand→metal σ-donation and metal→ligand π-back-donation in transition-metal complexes has been supported by quantum-chemical calculations, and formulas for the relative amounts of σ-donation and π-back-donation have been given, which make it possible to classify ligands on the basis of quantum chemically derived values.[8]

Transition-metal carbonyl complexes have been the subject of numerous accurate theoretical studies in the recent past, because not only is this class of compounds very important for experimental chemistry but it is also the archetype for understanding metal−ligand interactions.[5,6,9−12] Among the ubiquitous metal carbonyl complexes, there is a small but steadily increasing number of carbonyls which are peculiar, because the average value for the C−O stretching frequency ν(CO) is *higher* than for free CO (2143 cm^{-1}).[13,14] This subset of carbonyl complexes has been termed nonclassical metal carbonyls by Strauss.[13a,15] Most transition-metal carbonyls have CO stretching frequencies ν(CO) <2143 cm^{-1}, which is explained by the metal→CO π-back-donation into the π*(CO) orbital. It was suggested that in nonclassical carbonyls, which in most cases have positively charged metal atoms, OC→metal σ-donation and Coulombic attraction are the dominant binding forces and metal→CO π-back-donation is unimportant.[13a,15] A recent detailed discusion of the bonding model for nonclassical carbonyls suggests that, when a CO ligand approaches a positively charged transition metal, the C−O distance decreases and the CO bond energy and CO stretching frequency increase first as a result of σ-bonding interactions between M$^+$ and CO.[13a] Metal→CO π-back-donation becomes effective at a shorter M$^+$−CO distance, which leads to a turning point along the M$^+$−CO coordinate. This is schematically shown in Figure 1. This model is in agreement with earlier Hartree−Fock calculations of Cr(CO)$_6$ reported by Sherwood and Hall.[16] These authors calculated the energy gradient of the bond length of a CO ligand as a function of the (CO)$_5$Cr−CO distance. At short and normal Cr−C bond lengths, the CO bond length was predicted to be longer than that of free CO, while at long Cr−C distances the CO bond length should become shorter than in free CO.[16] The model was recently supported by quantum-mechanical calculations of M(CO)$^+$ (M = Cu, Ag, Au), which showed that the C−O bond length decreases first before it becomes longer at shorter M$^+$−CO distances.[18] It has also been shown that the C−O bond shortening upon approach of a positively charged atom is *not* due to the HOMO of CO having antibonding character.[17,18] Rather, the positive charge reduces the polarization of the C−O molecular orbitals and particularly the π orbitals, which leads to a more covalent and stronger C−O bond.[18]

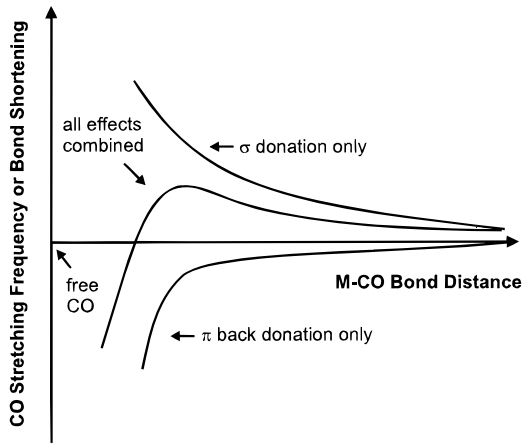

Figure 1. Effect of OC→metal σ-donation and M→CO π-back-donation on the C−O bond.

The present work was stimulated by the recent report of Willner, Aubke, and co-workers[14] about the synthesis, structure, and spectroscopic constants of the triply charged iridium carbonyl complex [Ir(CO)$_6$]$^{3+}$. The experimental results make it possible to compare the set of isoelectronic compounds [Hf(CO)$_6$]$^{2-}$, [Ta(CO)$_6$]$^-$, W(CO)$_6$, [Re(CO)$_6$]$^+$, [Os(CO)$_6$]$^{2+}$, and [Ir(CO)$_6$]$^{3+}$. Theoretical calculations can provide missing information such as the metal−CO bond dissociation energies, which are known only for W(CO)$_6$.[19] The series of isoelectronic hexacarbonyls can be used to analyze the nature of the metal−CO bonding. The bonding model of Strauss[13] lets one expet a trend from classical carbonyl complex toward a nonclassical carbonyl from [Hf(CO)$_6$]$^{2-}$ to [Ir(CO)$_6$]$^{3+}$, which is in agreement with the experimentally observed increase in the t_{1u} stretching mode of CO from [Hf(CO)$_6$]$^{2-}$ (1757 cm^{-1})[20] to [Ir(CO)$_6$]$^{3+}$ (2254 cm^{-1}).[14] However, the division of metal carbonyls into classical and nonclassical carbonyl complexes has been criticized by Willner, Aubke, and co-workers, who called it "arbi-

(6) Dapprich, S.; Frenking, G. *J. Phys. Chem.* **1995**, *99*, 9352.
(7) (a) Dewar, M. J. S.; *Bull. Soc. Chim. Fr.* **1951**, *18*, C79. (b) Chatt, J.; Duncanson, L. A. *J. Chem. Soc.* **1953**, 2929.
(8) (a) Dapprich, S.; Frenking, G. *Angew. Chem.* **1995**, *107*, 383; *Angew. Chem., Int. Ed. Engl.* **1995**, *34*, 354. (b) Ehlers, A. W.; Dapprich, S.; Vyboishchikov, S. F.; Frenking, G. *Organometallics* **1996**, *15*, 105. (c) Dapprich, S.; Frenking, G. *Organometallics* **1996**, *15*, 4547. (d) Antes, I.; Dapprich, S.; Frenking, G.; Schwerdtfeger, P. *Inorg. Chem.* **1996**, *35*, 2089.
(9) (a) Ehlers, A. W.; Frenking, G. *J. Am. Chem. Soc.* **1994**, *116*, 1514. (b) Ehlers, A. W.; Frenking, G. *Organometallics* **1995**, *14*, 423. (c) Ehlers, A. W.; Dapprich, S.; Vyboishchikov, S. F.; Frenking, G. *Organometallics* **1996**, *15*, 105.
(10) (a) Rosa, A.; Ehlers, A. W.; Baerends, E. J.; Snijders, J. G.; te Velde, G. *J. Phys. Chem.* **1996**, *100*, 5690. (b) Li, J.; Schreckenbach, G.; Ziegler, T. *J. Am. Chem. Soc.* **1995**, *117*, 486. (c) Li, J.; Schreckenbach, G.; Ziegler, T. *J. Phys. Chem.* **1994**, *98*, 4838.
(11) (a) Jonas, V.; Thiel, W. *J. Chem. Phys.* **1996**, *105*, 3636. (b) Jonas, V.; Thiel, W. *J. Chem. Phys.* **1995**, *102*, 8474.
(12) (a) Blomberg, M. R. A.; Siegbahn, P. E. M.; Lee, T. J.; Rendell, A. P.; Rice, J. E. *J. Chem. Phys.* **1991**, *95*, 5898. (b) Bérces, A. *J. Phys. Chem.* **1996**, *100*, 16538. (c) van Wüllen, Ch. *J. Chem. Phys.* **1996**, *105*, 5485.
(13) (a) Hurlburt, P. K.; Rack, J. J.; Luck, J. S.; Dec, S. F.; Webb, J. D.; Anderson, O. P.; Strauss, S. H. *J. Am. Chem. Soc.* **1994**, *116*, 10003. (b) Rack, J. J.; Webb, J. D.; Strauss, S. H. *Inorg. Chem.* **1996**, *35*, 277. (c) Selg, P.; Brintzinger, H. H.; Andersen, R. A.; Horváth, I. T. *Angew. Chem.* **1995**, *107*, 877; *Angew. Chem., Int. Ed. Engl.* **1995**, *34*, 791. (d) Guo, Z.; Swenson, D. C.; Guram, A. S.; Jordan, R. F. *Organometallics* **1994**, *13*, 766. (e) Hwang, G.; Wang, C.; Aubke, F.; Willner, H.; Bodenbinder, M. *Can. J. Chem.* **1993**, *71*, 1532. (f) Willner, H.; Bodenbinder, M.; Wang, C.; Aubke, F. *J. Chem. Soc., Chem. Commun.* **1994**, 1189. (g) Aubke, F.; Wang, C. *Coord. Chem. Rev.* **1994**, *137*, 483.
(14) Bach, C.; Willner, H.; Wang, C.; Rettig, S. J.; Trotter, J.; Aubke, F. *Angew. Chem.* **1996**, *108*, 2104; *Angew. Chem., Int. Ed. Engl.* **1996**, *35*, 1974.
(15) Strauss, S. H. *Chemtracts: Inorg. Chem.* submitted for publication.
(16) Sherwood, D. E.; Hall, M. B. *Inorg. Chem.* **1983**, *22*, 93.
(17) Goldman, A. S.; Krogh-Jespersen, K. *J. Am. Chem. Soc.* **1996**, *118*, 12159.
(18) Lupinetti, A.; Fau, S.; Frenking, G.; Strauss, S. H. *J. Am. Chem. Soc.*, submitted for publication.
(19) Lewis, K. E.; Golden, D. M.; Smith, G. P. *J. Am. Chem. Soc.* **1984**, *106*, 3905.
(20) Ellis, J. E.; Chi, K. M. *J. Am. Chem. Soc.* **1990**, *112*, 6022.

trary, not suitable and misleading".[14] We wanted to know whether the bonding model of Strauss is suitable to classify the isoelectronic hexacarbonyls according to his definition of classical and nonclassical carbonyls.[13]

In this paper we report about theoretically predicted geometries, metal−CO dissociation energies, and vibrational frequencies of the title compounds. The metal−CO bonding interactions have been analyzed using the recently developed charge decomposition analysis (CDA).[6] Atomic partial charges were calculated with the natural bond orbital (NBO) partitioning scheme developed by Weinhold.[21]

Methods

A 6-31G(d) basis set[22] for carbon and oxygen in conjunction with a quasi-relativistic small-core ECP for the metals with a (441/2111/21) valence basis set for the 14 outermost core and valence electrons has been used in this study.[23] This is our standard basis set combination II.[2a] The bond energies of the negatively charged species have also been calculated using basis set II augmented with a set of diffuse s and p functions at carbon and oxygen[24a] and two sets of f functions at the metal. The exponents of the first set of f functions have been optimized by us.[24b] The second set of f functions has been derived from the first set by multiplying the exponents with a factor of 0.1.

The geometries of the molecules have been optimized with O_h symmetry for the ($^1A_{1g}$) state of the hexacarbonyls and with C_{4v} symmetry for the $^1A_1$ state of the pentacarbonyls, with the exception of $[Hf(CO)_5]^{2-}$, which has a C_2-symmetric (^1A) singlet state. The optimizations were carried out at the level of Møller−Plesset second-order perturbation theory (MP2)[25] and gradient-corrected density functional theory (DFT). Gradient corrections for exchange and correlation energy were taken from the work of Becke[26a] and Perdew,[26b] respectively (BP86). DFT calculations were also carried out using the mixed hybrid functional introduced by Becke, which is termed B3LYP.[27] It has been shown that B3LYP and QCISD(T) optimized geometries of neutral and cationic transition-metal complexes are quite similar.[28] The vibrational frequencies, force constants, and zero-point vibrational energies (ZPE) of the hexacarbonyls have been computed at MP2/II, BP86/II, and B3LYP/II. All optimized structures reported here have only positive eigenvalues of the Hessian matrix, i.e. they are minima on the potential energy surface. Vibrational frequency calculations of the pentacarbonyls have been carried out only at B3LYP/II but not at BP86/II and MP2/II. It can be assumed that the BP86/II and MP2/II optimized pentacarbonyl complexes are also energy minima, because the optimized structures have the same symmetry and have geometries similar to those of the B3LYP/II optimized pentacarbonyls. Improved total energies are calculated at the CCSD(T) level[29] using basis set II at geometries optimized at MP2/II. For the calculations of the geometries and vibrational frequencies the program package Gaussian 94[30] has been used. The CCSD(T) calculations have been performed using the program ACES II.[31]

Inspection of the metal−CO donor−acceptor interactions was performed using charge-decomposition analysis (CDA).[6] In the CDA method the (canonical, natural, or Kohn−Sham) molecular orbitals of the complex are expressed in terms of the MOs of appropriately chosen fragments. In the present case, the natural orbitals (NO) of the MP2/II wave functions and the Kohn−Sham orbitals of the DFT calculations are formulated in the CDA calculations as a linear combination of the MOs of CO and the pentacarbonyl fragment in the geometry of the hexacarbonyl complex. The orbital contributions are divided into three parts: (i) the mixing of the occupied MOs of CO and the unoccupied MOs of the pentacarbonyl (σ-donation $OC\rightarrow M(CO)_5^q$), (ii) the mixing of the unoccupied MOs of CO and the occupied MOs of the pentacarbonyl (π-backdonation $(CO)_5M^q\rightarrow CO$), and (iii) the mixing of the occupied MOs of CO and the occupied MOs of the pentacarbonyl (repulsive polarization $OC\leftrightarrow M(CO)_5^q$). A more detailed presentation of the method and the interpretation of the results is given in ref 6. The CDA calculations have been performed using the program CDA 2.1.[32]

Results and Discussion

The geometries of the hexacarbonyls have been optimized under the restriction of O_h symmetry. Subsequent frequency calculations showed that the octahedral structures are indeed minima on the potential energy surfaces (number of imaginary frequencies $i = 0$). Table 1 shows the calculated and experimental bond lengths of the hexacarbonyls. At all levels of theory it is predicted that the M−CO bond length decreases from $[Hf(CO)_6]^{2-}$, which has the longest metal−CO bond, to $[Re(CO)_6]^+$, which has the shortest M−CO bond at the DFT level. Attempts to calculate $[Hf(CO)_6]^{2-}$ at MP2/II failed, because the geometry optimization did not converge. The metal−CO bond becomes slightly longer in $[Os(CO)_6]^{2+}$ than in $[Re(CO)_6]^+$ at the DFT level, while it remains nearly unchanged at MP2/II. $[Ir(CO)_6]^{3+}$ is calculated to have a longer metal−CO bond than $[Os(CO)_6]^{2+}$. The C−O bond lengths are calculated to become shorter from the dianion $[Hf(CO)_6]^{2-}$ to the trication $[Ir(CO)_6]^{3+}$.

The differences among the theoretically predicted M−CO bond lengths at B3LYP/II, BP86/II, and MP2/II are not very large. MP2/II optimized metal−CO bonds are always shorter than at BP86/II, which in turn are shorter than at B3LYP/II. The theoretical M−CO bond lengths are in good agreement with available experimental data (Table 1). We want to point out that the

(21) Reed, A. E.; Curtiss, L. A.; Weinhold, F. *Chem. Rev.* **1988**, *88*, 899.
(22) Hehre, W. J.; Ditchfield, R.; Pople, J. A. *J. Chem. Phys.* **1972**, *56*, 2257.
(23) Hay, P. J.; Wadt, W. R. *J. Chem. Phys.* **1985**, *82*, 299.
(24) (a) Clark, T.; Chandrasekhar, J.; Spitznagel, G. W.; Schleyer, P. v. R. *J. Comput. Chem.* **1983**, *4*, 294. (b) Ehlers, A. W.; Böhme, M.; Dapprich, S.; Gobbi, A.; Höllwarth, A.; Jonas, V.; Köhleer, K. F.; Stegmann, R.; Veldkamp, A.; Frenking, G. *Chem. Phys. Lett.* **1993**, *208*, 111.
(25) Møller, C.; Plesset, M. S. *Phys. Rev.* **1934**, *46*, 618. (b) Binkley, J. S.; Pople, J. A. *Int. J. Quantum Chem.* **1975**, *9*, 229.
(26) (a) Becke, A. D. *Phys. Rev. A* **1988**, *38*, 3098. (b) Perdew, J. P. *Phys. Rev. B* **1986**, *33*, 8822; **1986**, *34*, 7046.
(27) (a) Becke, A. D. *J. Chem. Phys.* **1993**, *98*, 5648. (b) Stevens, P. J., Devlin, F. J.; Chablowski, C. F.; Frisch, M. J. *J. Phys. Chem.* **1994**, *98*, 11623.
(28) Schröder, D.; Fiedler, A.; Schwarz, H. *Int. J. Mass Spectrom. Ion Processes* **1994**, *134*, 239.
(29) (a) Cizek, J. *J. Chem. Phys.* **1966**, *45*, 4256. (b) Cizek, J. *Adv. Chem. Phys.* **1966**, *14*, 35. (c) Pople, J. A.; Krishnan, R.; Schlegel, H. B.; Binkley, J. S. *Int. J. Quantum Chem.* **1978**, *14*, 545. (d) Bartlett, R. J.; Purvis, G. D. *Int. J. Quantum Chem.* **1978**, *14*, 561. (e) Purvis, G. D.; Bartlett, R. J. *J. Chem. Phys.* **1982**, *76*, 1910. (f) Purvis, G. D.; Bartlett, R. J. *J. Chem. Phys.* **1987**, *86*, 7041.
(30) Frisch, M. J.; Trucks, G. W.; Schlegel, H. B.; Gill, P. M. W.; Johnson, B. G.; Robb, M. A.; Cheeseman, J. R.; Keith, T. A.; Petersson, G. A.; Montgomery, J. A.; Raghavachari, K.; Al-Laham, M. A.; Zakrzewski, V. G.; Ortiz, J. V.; Foresman, J. B.; Cioslowski, J.; Stefanov, B. B.; Nanayakkara, A.; Challacombe, M.; Peng, C. Y.; Ayala, P. Y.; Chen, W.; Wong, M. W.; Andres, J. L.; Replogle, E. S.; Gomberts, R.; Martin, R. L.; Fox, D. J.; Binkley, J. S.; Defrees, D. J.; Baker, I.; Stewart, J. J. P.; Head-Gordon, M.; Gonzalez, C.; Pople, J. A. Gaussian 94; Gaussian Inc., Pittsburgh, PA, 1995.
(31) ACES II, an ab initio program system written by J. F. Stanton, J. Gauss, J. D. Watts, W. J. Lauderdale and R. J. Bartlett, University of Florida, Gainesville, FL, 1991.
(32) CDA 2.1 by S. Dapprich and G. Frenking, 1994. The program is available via anonymous ftp server: ftp.chemie.uni-marburg.de (/pub/cda).

Table 1. Calculated and Experimental Bond Lengths (Å) of the Hexacarbonyl Complexes and CO

compd	M−C	C−O	method
$[Hf(CO)_6]^{2-}$ (O_h)	2.211	1.182	B3LYP
	2.206	1.196	BP86
	2.174(3); 2.179(3); 2.180(3)	1.162(5); 1.165(4); 1.162(4)	X-ray[a]
$[Ta(CO)_6]^-$ (O_h)	2.124	1.166	B3LYP
	2.118	1.179	BP86
	2.113	1.180	MP2
	2.083(6)	1.149(8)	X-ray[b]
$W(CO)_6$ (O_h)	2.074	1.151	B3LYP
	2.066	1.164	BP86
	2.060	1.166	MP2
	2.058	1.148	ED[c]
	2.018; 2.025; 2.032; 2.033	1.130; 1.139; 1.152; 1.158	X-ray[d]
$[Re(CO)_6]^+$ (O_h)	2.046	1.138	B3LYP
	2.036	1.151	BP86
	2.026	1.155	MP2
	1.98(3); 2.03(6); 2.02(6); 1.89(7); 2.07(7)	1.14(4); 1.12(7); 1.16(8); 1.19(8); 1.12(9)	X-ray[e]
$[Os(CO)_6]^{2+}$ (O_h)	2.049	1.128	B3LYP
	2.038	1.141	BP86
	2.025	1.148	MP2
$[Ir(CO)_6]^{3+}$ (O_h)	2.068	1.121	B3LYP
	2.057	1.135	BP86
	2.041	1.144	MP2
	2.05(1); 2.01(1); 2.04(1); 2.00(2); 2.02(2);	1.07(1); 1.08(2); 1.12(2)	X-ray[f]
CO ($C_{\infty v}$)		1.150	B3LYP
		1.138	BP86
		1.152	MP2
		1.143	exptl[g]

[a] Reference 37a. [b] Reference 37b. [c] Reference 35. [d] Reference 37c. [e] References 37d,e. [f] Values for $[Ir(CO)_5Cl]^{2+}$.[14] [g] Reference 34.

gas-phase value for the $(OC)_5W-CO$ bond length is clearly longer than the X-ray value. The difference can be attributed to solid-state effects and inherent errors of the approximations in the X-ray structure analysis. Since the X-ray values for the M−CO bond lengths are always slightly shorter than the calculated values, it should be expected that the theoretically predicted metal−CO bond lengths reflect the gas-phase values for the free hexacarbonyls with high accuracy.

Table 2 shows the calculated bond lengths and bond angles of the pentacarbonyls. As in the hexacarbonyl case, geometry optimization at MP2/II of $[Hf(CO)_5]^{2-}$ failed because the optimization procedure did not converge. The equilibrium geometry of $[Hf(CO)_5]^{2-}$ predicted at B3LYP/II and BP86/II has C_2 symmetry, while the other pentacarbonyls have C_{4v} symmetry. The C_2-symmetric equilibrium structure of $[Hf(CO)_5]^{2-}$ is only slightly distorted from the C_{4v} form. The M−CO bonds of the pentacarbonyls trans to the empty site are clearly shorter than in the respective hexacarbonyl, while the cis M−CO bonds change only slightly.

Table 3 shows the calculated first dissociation energies (FDEs) of a CO ligand from the hexacarbonyls. The only experimental value of the hexacarbonyls investigated here has been reported for $W(CO)_6$. The experimental result[19] $D_0 = 46.0 \pm 2$ kcal/mol is in excellent agreement with the CCSD(T) value of 45.9 kcal/mol, while the MP2/II result (52.7 kcal/mol) is too high. This result has been published before.[9] Both DFT methods give dissociation energies for $W(CO)_6$ which are within the experimental error range.

Table 2. Calculated Bond Lengths (Å) and Bond Angles (deg) of the Pentacarbonyl Complexes

complex	M−C[a]	C−O[a]	$C_{api}-M-C_{eq}$	M−C−O	method
$[Hf(CO)_5]^{2-}$ (C_2)	2.129	1.191			B3LYP
	2.190	1.188	103.29	173.35	
	2.195	1.190	80.02	173.41	
	2.119	1.205			BP86
	2.190	1.206	101.40	174.07	
	2.185	1.203	81.68	173.99	
$[Ta(CO)_5]^-$ (C_{4v})	2.021	1.177	89.97	178.25	B3LYP
	2.111	1.170			
	2.014	1.190	90.16	178.42	BP86
	1.190	1.185			
	2.016	1.189	85.84	174.56	MP2
	2.097	1.185			
$W(CO)_5$ (C_{4v})	1.959	1.161	90.72	179.02	B3LYP
	2.065	1.153			
	1.951	1.174	90.81	179.19	BP86
	2.057	1.167			
	1.944	1.179	88.90	176.98	MP2
	2.054	1.168			
$[Re(CO)_5]^+$ (C_{4v})	1.920	1.146	91.26	179.80	B3LYP
	2.045	1.138			
	1.909	1.160	91.29	179.85	BP86
	2.033	1.152			
	1.890	1.166	90.27	178.33	MP2
	2.029	1.155			
$[Os(CO)_5]^{2+}$ (C_{4v})	1.917	1.133	91.74	179.51	B3LYP
	2.055	1.127			
	1.903	1.148	91.83	179.34	BP86
	2.041	1.141			
	1.886	1.154	91.22	179.72	MP2
	2.037	1.147			
$[Ir(CO)_5]^{3+}$ (C_{4v})	1.912	1.139	92.24	178.26	B3LYP
	2.068	1.135			
	1.928	1.124	92.04	178.58	BP86
	2.081	1.121			
	1.903	1.147	91.52	179.07	MP2
	2.059	1.144			

[a] The first value denotes the apical bond, and the next values denote the equatorial bonds.

At all levels of theory it is predicted that the trication $[Ir(CO)_6]^{3+}$ has the highest FDE (Table 3). There is a significant decrease in the calculated FDE values from $[Ir(CO)_6]^{3+}$ to $[Os(CO)_6]^{2+}$ and to $[Re(CO)_6]^+$. It follows that a positive charge at the metal enhances the FDE of the hexacarbonyls. The FDEs of $[Re(CO)_6]^+$, $W(CO)_6$, and $[Ta(CO)_6]^-$ are not very different. The lowest FDE calculated at the CCSD(T) and MP2/II level is found for $[Ta(CO)_6]^-$, while the DFT methods predict that the neutral hexacarbonyl $W(CO)_6$ should have the lowest FDE. All theoretical methods predict that $[Hf(CO)_6]^{2-}$ has a higher FDE than $[Ta(CO)_6]^-$ (Table 3). In order to make sure that the higher FDE of $[Hf(CO)_6]^{2-}$ compared to that of $W(CO)_6$ is not an artifact of the basis set II, which does not have diffuse functions, we calculated the FDE of $[Hf(CO)_6]^{2-}$, $[Ta(CO)_6]^-$, and $W(CO)_6$ at the BP86 level using an extended basis II+D set which includes diffuse s and p functions at carbon and oxygen and two sets of f functions at the metal. Details of the basis set are given in Methods. The calculated dissociation energies at BP86/II+D using BP86/II optimized geometries are $D_e = 51.04$ kcal/mol for $[Hf(CO)_6]^{2-}$, $D_e = 48.71$ kcal/mol for $[Ta(CO)_6]^-$, and $D_e = 47.36$ kcal/mol for $W(CO)_6$. The calculated FDEs using the extended basis set have the same trend and are very similar to the results shown in Table 3. It follows that the higher FDE of $[Hf(CO)_6]^{2-}$ compared with $W(CO)_6$ is also predicted using larger basis sets.

Table 3. Calculated and Experimental First Dissociation Energies D_e (kcal mol^{-1})[a]

method	$[Hf(CO)_6]^{2-}$	$[Ta(CO)_6]^{-}$	$W(CO)_6$	$[Re(CO)_6]^{+}$	$[Os(CO)_6]^{2+}$	$[Ir(CO)_6]^{3+}$
B3LYP	51.40 (49.61)	47.81 (45.95)	45.93 (43.84)	48.22 (45.99)	58.20 (55.87)	74.94 (72.59)
BP86	54.86 (53.18)	50.94 (49.08)	49.43 (47.34)	52.25 (50.02)	62.57 (60.24)	79.05 (76.70)
MP2		53.08 (51.21)	54.76 (52.67)	58.21 (55.98)	69.90 (67.27)	85.71 (83.36)
CCSD(T)[b]		47.94 (46.07)	48.02 (45.93)	50.57 (48.34)	60.95 (58.62)	77.45 (75.10)
exptl[c]			46.0 ± 2			

[a] ZPE corrected D_0 values are given in parentheses. The ZPE corrections are taken from B3LYP calculations. [b] Using MP2-optimized geometries. [c] Reference 19.

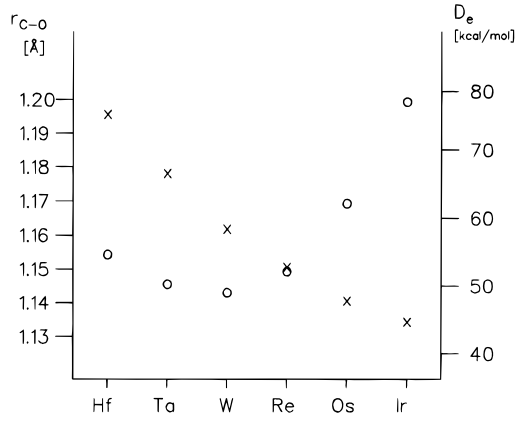

Figure 2. Plot of the calculated CO bond dissociation energies D_e (○) and C−O equilibrium distances (×) of the hexacarbonyls at the BP86/II level.

Figure 2 shows the calculated trend for the C−O bond lengths and the FDEs of the hexacarbonyls. It becomes obvious that there is no correlation between the two properties. Although $[Hf(CO)_6]^{2-}$ has the largest metal→CO π-back-donation (see below), yielding the longest C−O bond of the hexacarbonyls, it has a weaker FDE than $[Os(CO)_6]^{2+}$ and particularly $[Ir(CO)_6]^{3+}$. This is remarkable, because π-back-donation has been found to be the dominant contribution to the metal−CO bond energy in neutral carbonyl complexes.[5] The calculated bond energies disprove the assumption that nonclassical metal carbonyls, which are mainly bonded by OC→M σ-donation and Coulombic attraction, are weakly bound species. The nonclassical complex $[Ir(CO)_6]^{3+}$ has the highest FDE of all hexacarbonyls investigated here. An explanation for this is given below.

Table 4 shows the calculated and experimental vibrational frequencies and force constants for the C−O stretching modes of the hexacarbonyls. Theory predicts that the Raman-active e_g and a_{1g} vibrations and the IR-active t_{1u} vibration show a trend with increasing wavenumbers and force constants from $[Hf(CO)_6]^{2-}$ to $[Ir(CO)_6]^{3+}$. A complete set of experimental vibrational frequencies is only available for the asymmetric CO stretching mode. Figure 3 shows a plot of the calculated and experimental wavenumbers for the t_{1u} vibrations of the hexacarbonyls. The experimental and theoretical values at all levels of theory show the same trend. The calculated absolute values of the vibrational frequencies using BP86/II agree quite well with the experimental results, while the B3LYP/II frequencies are always too high. The good performance of the BP86/II level of theory for calculating vibrational frequencies of transition-metal carbonyls has been noted before by Jonas and Thiel.[11]

Table 4. Calculated and Experimental Carbonyl Stretching Frequencies ν_{CO} (cm^{-1}) and Force Constants F_{CO} (mdyn Å^{-1}) of the Hexacarbonyl Complexes and CO

	T_{1u}[a]		E_g[b]	A_{1g}[c]	
compd	ν_{CO}	F_{CO}	ν_{CO}	ν_{CO}	method
$[Hf(CO)_6]^{2-}$	1863.3	14.50	1873.8	1990.9	B3LYP
	1798.5	13.49	1805.4	1910.3	BP86
	1757				exptl[d]
$[Ta(CO)_6]^{-}$	1969.7	16.22	1988.7	2098.6	B3LYP
	1899.4	15.06	1914.6	2015.6	BP86
	1896.4	14.75	1882.9	2019.2	MP2
	1850				exptl[e]
$W(CO)_6$	2074.2	18.00	2097.7	2191.8	B3LYP
	1996.4	16.65	2017.3	2106.7	BP86
	1977.7	16.35	1998.5	2095.1	MP2
	1977	17.0[f]	1998	2115	exptl[g]
$[Re(CO)_6]^{+}$	2176.6	19.83	2200.1	2271.9	B3LYP
	2088.8	18.24	2112.4	2184.2	BP86
	2053.1	17.64	2087.2	2148.1	MP2
	2085	18.1[f]	2122	2197	exptl[h]
$[Os(CO)_6]^{2+}$	2267.5	21.50	2287.4	2333.1	B3LYP
	2165.7	19.60	2187.0	2237.3	BP86
	2113.9	18.67	2144.1	2172.7	MP2
	2190	19.8[f]	2218	2259	exptl[i]
$[Ir(CO)_6]^{3+}$	2335.2	22.77	2349.6	2373.4	B3LYP
	2223.5	20.65	2240.4	2269.3	BP86
	2139.6	19.09	2163.2	2167.9	MP2
	2254	20.8[f]	2276	2295	exptl[j]
CO[k]	2211.6	20.21			B3LYP
	2117.6	18.79			BP86
	2118.9	18.81			MP2
	2143	18.9			exptl[l]

[a] IR active, triply degenerate. [b] Raman active, doubly degenerate. [c] Raman-active mode. [d] Reference 37a. [e] Reference 37f. [f] Calculated by the Cotton−Krainhanzel method.[38] [g] Reference 37g. [h] Reference 37h. [i] Reference 37i. [j] Reference 14. [k] IR active, S_g mode. [l] Reference 34.

In order to get an understanding of the differences and the trend of the metal−CO bonding of the hexacarbonyls in terms of chemical models, we analyzed the calculated data using decomposition schemes. Because there have only been a few reports where results obtained from the analysis of DFT calculations and classical quantum-chemical methods are compared, we report on a comparative analysis of the DFT and MP2 results. Table 5 shows calculated partial charges of the hexacarbonyls using the NBO method. At all levels of theory it is predicted that the metal atoms carry a negative partial charge, except for the iridium atom in $[Ir(CO)_6]^{3+}$. It is interesting to note that Ta, W, and

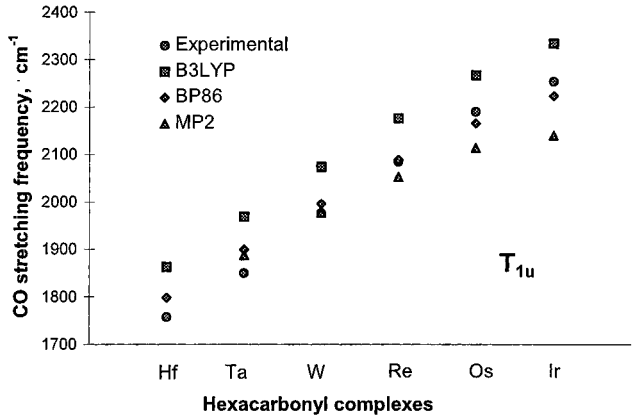

Figure 3. Plot of the calculated and experimental IR-active (t_{1u}) CO stretching frequencies of the hexacarbonyls.

even Re are calculated to carry a higher negative charge than Hf, although the Hf complex has a total charge of −2. This indicates that the Hf→CO π-back-donation should be quite effective. The partial charges for the metal atoms calculated at the DFT level are more negative than the MP2 charges, but the trend is the same, except for the sequence $[Ta(CO)_6]^-/W(CO)_6$.

Table 6 shows the results of the CDA method for the hexacarbonyls. The OC→metal σ-donation is always larger than the metal→CO π-back-donation. We want to point out that the absolute numbers for the calculated σ-donation and π-back-donation are not very meaningful. More important is the *ratio* of the σ-donation and π-back-donation, which gives the relative weights of the two donor−acceptor components. Also, the difference between the σ-donation and π-back-donation cannot be used as a measure of the charge exchange. The third term, denoted "repulsive polarization", which gives the contribution from the mixing of the occupied orbitals of the ligand and the metal, indicates by its negative spin that electronic charge is removed from the overlapping area of the occupied orbitals. However, there is no information as to where the charge is going, which makes the CDA results not suitable for calculating partial charges.

The results shown in Table 6 indicate that, upon going from $[Hf(CO)_6]^{2-}$ to $[Ir(CO)_6]^{3+}$, there is a gradual decrease of the relative importance of the M→CO π-back-donation. The contribution of the M→CO π-back-donation to the total donation decreases from ∼42% for $[Hf(CO)_6]^{2-}$ (note the remarkably similar ratios at B3LYP/II, BP86/II, and MP2/II) to 8% at B3LYP/II and 10% at BP86/II for $[Ir(CO)_6]^{3+}$. The MP2/II calculations give no metal→CO π-back-donation in $[Ir(CO)_6]^{3+}$. Figure 4a shows a plot of the percent back-donation and the theoretically predicted shift of the CO stretching frequencies for the hexacarbonyls calculated at B3LYP/II. It becomes obvious that the CO stretching frequency decreases when the M→CO π-back-donation becomes larger. Figure 4a strongly supports the postulate that the decrease in the CO stretching frequency indicates more metal→CO π-back-donation. Some caution is advisable, however, when one tries to correlate directly the calculated or observed CO stretching frequency or force constant with the amount of metal−CO π-back-donation. It has been shown that the C−O stretching frequency may be strongly influenced by coupling with other modes.[17,18] This makes the vibrational spectra less suitable as an indicator for metal−CO interactions. A better choice are the C−O bond lengths, which are difficult to measure, however. Figure 4b shows a plot of the calculated C−O bond lengths and the percent M→CO π-back-donation. It becomes obvious that a larger donation from the occupied d orbitals of the metal into the π^*(CO) orbital leads to a longer C−O bond, which becomes quite long in $[Hf(CO)_6]^{2-}$. This result is in agreement with generally accepted models about transition-metal−ligand interactions. The relevance of the results presented here is that they are obtained from the analysis of a quantum-chemical calculation, which gives accurate geometries, vibrational frequencies, and bond energies without making an assumption about the nature of the metal−ligand interactions.

In order to investigate the model for metal−CO interactions introduced by Strauss,[13a,15] which is schematically shown in Figure 1, we calculated at the B3LYP/II level of theory the change of the C−O bond length when the metal−CO bonds of the hexacarbonyls are stretched. We have chosen $[Hf(CO)_6]^{2-}$, $W(CO)_6$, and $[Ir(CO)_6]^{3+}$ as examples. $Cr(CO)_6$ has also been included in order to compare the results with the previous work of Sherwood and Hall (SH).[16] Figure 5 shows the plots of the B3LYP/II optimized C−O bond lengths at different distances M−CO (i) when a single M−CO bond is stretched up to 2.0 Å from the equilibrium bond length and (ii) when the symmetry is constrained to O_h, i.e. when all six M−CO bonds become longer. Figure 5a shows that the C−O bond of $[Hf(CO)_6]^{2-}$ becomes shorter at longer metal−CO distances, but it never becomes shorter than in free CO. This holds true for single and multiple CO dissociation. Even when the metal−CO distance is stretched by 2.0 Å, the bond length of the leaving CO (1.1630 Å for multiple CO dissociation, 1.1564 Å for single CO dissociation) is still significantly longer than in free CO (1.1377 Å). This result is apparently in conflict with the calculations of SH[16] and the model of Strauss,[15] which predict shorter C−O bond lengths at longer metal−CO distances. However, the HOMO of the dianion $[Hf(CO)_6]^{2-}$ is very diffuse, because it is occupied by two weakly bonded electrons which have been added to the neutral compound. The Hf→CO π-back-donation can therefore compete with the OC→Hf σ-donation even at longer Hf−CO distances. This assumption is supported by the analysis of the $(CO)_5Hf^-$−CO interactions (single dissociation[33]) using the CDA method. Table 7 shows that the OC→Hf σ-donation and the Hf→CO π-back-donation decrease at longer Hf−CO distances but the *ratio* of the two components of the charge donation remains nearly the same until the bond is stretched by 0.5 Å. There is still a significant contribution of the π-back-donation

(33) The CDA results for multiple CO dissociation are similar to those for single dissociation. However, it is difficult and somewhat arbitrary to determine the proper electron configuration of the metal atom when the M−CO distance becomes longer. Therefore, we discuss the CDA results only for single CO dissociation.

(34) Huber, K. P.; Herzberg, G. P. *Constants of Diatomic Molecules*; Van Nostrand Reinhold: New York, 1970.

(35) Arnesen, S. V.; Seip, H. M. *Acta Chem. Scand.* **1966**, *20*, 2711.

(36) We also carried out a topological analysis of the electron density distribution[39] of the hexacarbonyl complexes. The calculations of the energy density at the bond critical point H_b of the metal−CO bond at B3LYP/II gave a smooth trend from $[Hf(CO)_6]^{2-}$ ($H_b = -0.053$ hartree/Å^3) to $[Ir(CO)_6]^{3+}$ ($H_b = -0.274$ hartree/Å^3). It has been suggested that covalent bonds have negative H_b values, while closed-shell interactions (ionic bonds or van der Waals bonds) have $H_b \geq 0$.[40] This means that from $[Hf(CO)_6]^{2-}$ to $[Ir(CO)_6]^{3+}$ the ionic character decreases and the covalent character increases.

Table 5. Calculated NBO Atomic Charges of the Hexacarbonyl Complexes

	B3LYP			BP86			MP2		
complex	M	C	O	M	C	O	M	C	O
$[Hf(CO)_6]^{2-}$	−0.66	0.36	−0.59	−0.57	0.32	−0.55			
$[Ta(CO)_6]^{-}$	−0.81	0.47	−0.50	−0.75	0.43	−0.47	−0.61	0.38	−0.45
$W(CO)_6$	−0.78	0.55	−0.42	−0.73	0.51	−0.39	−0.64	0.46	−0.36
$[Re(CO)_6]^{+}$	−0.67	0.61	−0.33	−0.65	0.57	−0.30	−0.59	0.53	−0.26
$[Os(CO)_6]^{2+}$	−0.25	0.61	−0.24	−0.26	0.58	−0.20	−0.21	0.54	−0.17
$[Ir(CO)_6]^{3+}$	0.24	0.60	−0.14	0.18	0.58	−0.11	0.26	0.53	−0.07

Table 6. Results of the Charge Decomposition Analyses of the Hexacarbonyl Complexes: $OC\rightarrow M(CO)_5$ Donation *d*, $(CO)_6M\rightarrow CO$ Back-Donation *b*, and $(CO)_6M\leftrightarrow CO$ Repulsive Polarization *r*

complex	*d*	*b*	*r*
	B3LYP		
$[Hf(CO)_6]^{2-}$	0.50	0.37 (42%)	−0.20
$[Ta(CO)_6]^{-}$	0.48	0.32 (40%)	−0.25
$W(CO)_6$	0.45	0.25 (35%)	−0.27
$[Re(CO)_6]^{+}$	0.45	0.18 (28%)	−0.26
$[Os(CO)_6]^{2+}$	0.48	0.11 (19%)	−0.23
$[Ir(CO)_6]^{3+}$	0.51	0.04 (8%)	−0.20
	BP86		
$[Hf(CO)_6]^{2-}$	0.53	0.37 (41%)	−0.20
$[Ta(CO)_6]^{-}$	0.50	0.33 (39%)	−0.25
$W(CO)_6$	0.47	0.25 (35%)	−0.28
$[Re(CO)_6]^{+}$	0.45	0.19 (29%)	−0.28
$[Os(CO)_6]^{2+}$	0.48	0.12 (20%)	−0.25
$[Ir(CO)_6]^{3+}$	0.50	0.05 (10%)	−0.22
	MP2		
$[Ta(CO)_6]^{-}$	0.36	0.28 (43%)	−0.28
$W(CO)_6$	0.34	0.18 (34%)	−0.32
$[Re(CO)_6]^{+}$	0.38	0.12 (24%)	−0.29
$[Os(CO)_6]^{2+}$	0.42	0.05 (11%)	−0.25
$[Ir(CO)_6]^{3+}$	0.46	0.00 (0%)	−0.21

when the bond is further stretched by up to 2.0 Å. The very long reach of the Hf→CO π-back-donation explains why there is a smooth decrease and no turning point of the CO bond length when the Hf−CO distance becomes longer.

Parts b and c of Figure 5 show also the results for $W(CO)_6$ and $Cr(CO)_6$. Unlike the case for $[Hf(CO)_6]^{-}$, there is a turning point in the calculated C−O distance when a single CO dissociates from $W(CO)_6$ or $Cr(CO)_6$. The C−O bond length of the neutral hexacarbonyls becomes shorter than in free CO at M−CO ≈ +0.4 Å for $W(CO)_6$ and M−CO ≈ +0.5 Å for $Cr(CO)_6$. The result for $Cr(CO)_6$ is in agreement with the previous study of SH.[16] Figure 5 shows that there is no turning point in the curve of the C−O distance when all six carbonyls dissociate from $W(CO)_6$ and $Cr(CO)_6$. The CDA results given in Table 7 show that the contribution of the M→CO π-back-donation of the neutral carbonyls

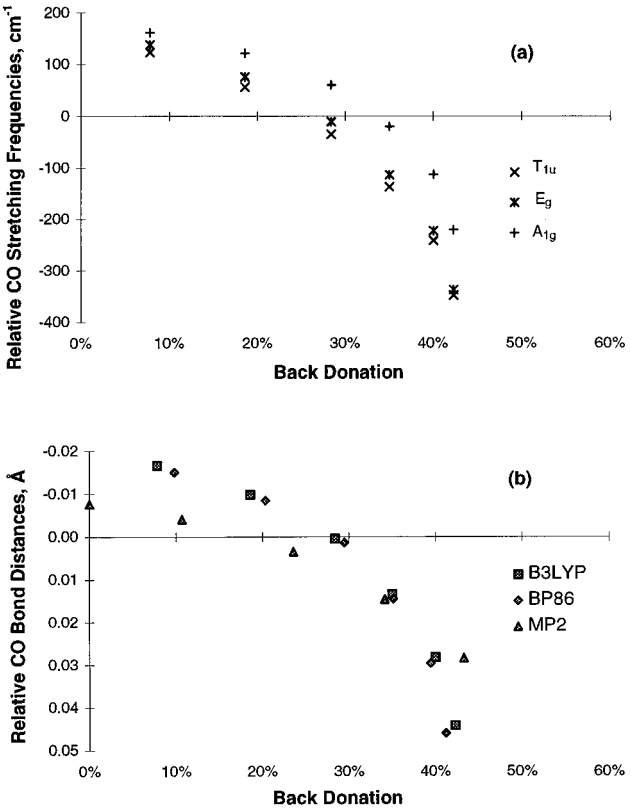

Figure 4. (a) Plot of the calculated percent M→CO π-back-donation given by the CDA method and the change of the theoretically predicted CO stretching frequencies relative to free CO calculated at the B3LYP/II level. (b) Plot of the calculated percent M−CO π-back-donation and the CO bond shortening (negative numbers) or lengthening (positive numbers) relative to free CO.

displays a steeper decrease than for $[Hf(CO)_6]^{-}$. At M−CO = +1.0 Å, there is only 12% back-donation in $W(CO)_6$ and 10% in $Cr(CO)_6$, while there is still 38% back-donation in $[Hf(CO)_6]^{-}$. At M−CO = +2.0 Å, the back-donation in the neutral hexacarbonyls is negligible, while there is still 28% back-donation in $[Hf(CO)_6]^{-}$.

The results for $[Ir(CO)_6]^{3+}$ are very interesting. The C−O bond length of $[Ir(CO)_6]^{3+}$ at the equilibrium geometry is shorter than in free CO (Table 1). Figure 5 shows that the C−O bond becomes at first even shorter when the Ir−CO bond is stretched. This holds for single and multiple CO dissociations, which have very similar curves. There is a turning point of the curve when the Ir−CO distance is stretched by ∼0.25 Å. After this, the C−O bond becomes longer and eventually approaches the value for free CO. Thus, $[Ir(CO)_6]^{3+}$ is an example for the case where the equilibrium M−CO bond length is only slightly shorter than the turning point of the C−O bond length as a function of the metal−CO distance. $[Ir(CO)_6]^{3+}$ is an example for a nonclassical carbonyl.[13a,15] It is surprising, how-

(37) (a) Ellis, J. E.; Chi, K.-M. *J. Am. Chem. Soc.* **1990**, *112*, 6022. (b) Calderazzo, F.; Englert, U.; Pampaloni, G.; Pelizzi, G.; Zamboni, R. *Inorg. Chem.* **1983**, *22*, 1865. (c) Heinemann, F.; Schmidt, H.; Peters, K.; Thiery, D. *Z. Kristallogr.* **1992**, *198*, 123. (d) Bruce, D. M.; Holloway, J. H.; Russel, D. R. *J. Chem. Soc., Dalton Trans.* **1978**, 1627. (e) Holloway, J. H.; Senior, J. B.; Szary, A. C. *J. Chem. Soc., Dalton Trans.* **1987**, 741. (f) Siebert, H. *Anwendungen der Schwingungsspektroskopie in der anorganischen Chemie*; Springer: Berlin, 1966. (g) Jones, L. H.; McDowell, R. S.; Goldblatt, M. *Inorg. Chem.* **1969**, *8*, 2349. (h) Abel, E. W.; McLean, R. A. N.; Tyfield, S. P.; Braterman, P. S.; Walker, A. P.; Hendra, P. J. *J. Mol. Spectrosc.* **1969**, *30*, 29. (i) Wang, C.; Bley, B.; Balzer-Jöllenbeck, G.; Lewis, A. R.; Siu, S. C.; Willner, H.; Aubke, F. *J. Chem. Soc., Chem. Commun.* **1995**, 2071.

(38) Cotton, F. A.; Kraihanzel, C. S. *J. Am. Chem. Soc.* **1962**, *84*, 4432.

(39) Bader, R. F. W. *Atoms in Molecules. A Quantum Theory*; Oxford University Press: New York, 1990.

(40) Cremer, D.; Kraka, E. *Angew. Chem.* **1984**, *96*, 612; *Angew. Chem., Int. Ed. Engl.* **1984**, *23*, 627.

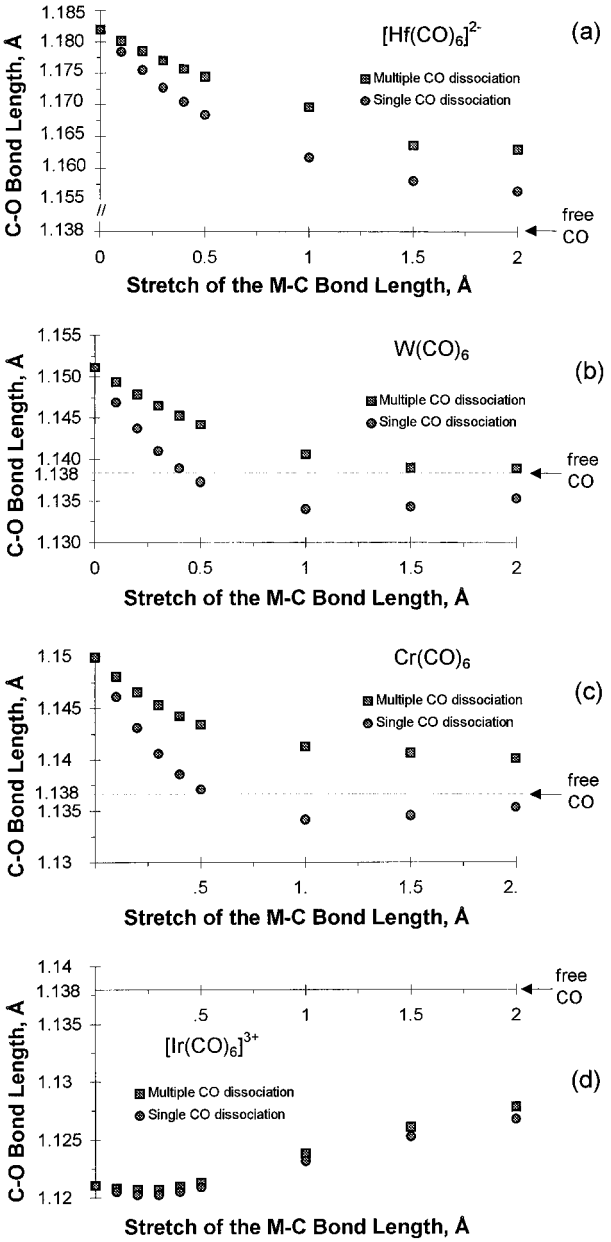

Figure 5. Calculated (B3LYP/II) CO bond lengths as a function of the metal−CO distance for single CO dissociation (circles) and for dissociation of all six CO groups (squares): (a) $[Hf(CO)_6]^{2-}$; (b) $W(CO)_6$; (c) $Cr(CO)_6$; (d) $[Ir(CO)_6]^{3+}$. The bond length of free CO calculated at the B3LYP/II level is 1.1377 Å.

ever, that the CO bond of the leaving carbonyls still becomes shorter in the beginning when the Ir−CO distance is stretched, because the CDA results suggest that Ir→CO π-back-donation in the equilibrium structure is not very strong, only 8% of the total donation (Table 6). Although the shortening of the C−O bond length is very small (only 0.0008 Å, see Table 7), it is enlightening to analyze the reason for the bond shortening.

Table 7 shows that the relative contribution of the π-back-donation decreases when the Ir−CO distance becomes longer. At the turning point there is only ∼5−6% Ir→CO π-back-donation left. It is tempting to suggest that the small amount of metal→CO π-back-donation is sufficient to overcome the C−O bond-shortening effect of the OC→M σ-donation. However, calculations at the MP2/II level give also at first a shortening of the C−O bond length when the Ir−CO distance becomes longer, although the CDA results at MP2/II using natural molecular orbitals give no Ir→CO π-back-donation (Table 6). An explanation for the small C−O bond shortening at longer M−CO distances in the absence of π-back-donation can be given when the third term of the CDA analysis is considered, i.e. the repulsive polarization *r*. This term describes the change in the electronic structure due to the interactions between occupied orbitals of the two fragments.[6] The repulsive polarization is always negative, because electronic charge is removed from the overlapping area of the two fragments. Figure 6 shows schematically the effect of the repulsive polarization on the shape of the occupied π orbital of CO. Removing charge from the overlapping area of the CO π orbitals with the occupied d(π) orbital of the metal leads to a more polarized CO π-bond, which weakens the CO bond. It follows that the OC→M σ-donation and M→CO π-back-donation has an effect on not only the C−O bond length but also the repulsive polarization OC↔M. This effect is usually not considered in the discussion of metal−ligand interactions. Table 7 shows that there is always a significant contribution of the repulsive polarization to the metal−CO interactions at the equilibrium geometry of the hexacarbonyls and that it is more important for $[Ir(CO)_6]^{3+}$ than π-back-donation. The repulsive polarization becomes clearly weaker when the Ir−CO distance is stretched by 0.2 Å, which contributes to the stretch of the C−O bond length. It is difficult to decide if the π-back-donation or the repulsive polarization has a stronger effect on the C−O bond length, but the small C−O shortening in the case of $[Ir(CO)_6]^{3+}$ seems to be caused by the latter term, because it is much larger than the π-back-donation.

The analysis of the metal−CO interactions makes it possible to give an explanation for the calculated trend of the FDEs of the hexacarbonyls. The large positive charge of the triply charged $[Ir(CO)_6]^{3+}$ and doubly charged $[Os(CO)_6]^{2+}$ causes the metals to become very good electron attractors. Table 5 shows that the total charge transfer from the six CO ligands to the metals is very large. At the B3LYP/II level, the charge transfer is 2.76 e for $[Ir(CO)_6]^{3+}$ and 2.25 e for $[Os(CO)_6]^{2+}$. Even the singly charged $[Re(CO)_6]^{+}$ has a charge transfer of 1.67 e from the ligands to the metal. This apparently compensates for the weak M→CO π-back-donation and leads to even higher FDEs for $[Ir(CO)_6]^{3+}$ and $[Os(CO)_6]^{2+}$ compared to $W(CO)_6$. Note that the highly charged $[Ir(CO)_6]^{3+}$ and $[Os(CO)_6]^{2+}$ have the lowest partial charges at the metal and the oxygen atoms and that even the positive charge at the carbon atoms is not very high (Table 5). This means that the large positive total charge is rather evenly distributed over the whole complex. The calculated charge distribution indicates that $[Ir(CO)_6]^{3+}$ has the most covalent metal−CO bond of the hexacarbonyls studied here.[36] The slightly higher FDE of $[Hf(CO)_6]^{2-}$ compared to $W(CO)_6$ can be explained by the strongly enhanced M→CO π-back-donation at longer Hf−CO distances, which is due to the energetically high-lying and diffuse d orbitals in the dianion. It becomes obvious that the strength of the metal−CO bond is determined by several factors, particularly when the carbonyl complex carries a positive or negative charge.

Table 7. Calculated CO Bond Lengths r_{C-O} (Å), OC→M(CO)$_5$ Donation *d*, (CO)$_5$M→CO Back-Donation *b*, and OC↔M(CO)$_5$ Repulsive Polarization *r* as a Function of the M−CO Distance at the B3LYP/II Level for Single CO Dissociation

	stretching of the M−CO bond, Å								
	0.0	0.1	0.2	0.3	0.4	0.5	1.0	1.5	2.0
				$[Hf(CO)_6]^{2-}$					
r_{C-O}	1.1819	1.1784	1.1755	1.1727	1.1705	1.1684	1.1617	1.158	1.1564
d	0.50	0.47	0.44	0.42	0.40	0.38	0.26	0.16	0.10
b	0.37	0.34	0.31	0.28	0.26	0.23	0.14	0.07	0.04
r	−0.20	−0.15	−0.12	−0.09	−0.07	−0.05	−0.02	−0.01	0.00
% back-donation	42	42	41	40	39	38	34	31	28
				$W(CO)_6$					
r_{C-O}	1.1511	1.1469	1.1437	1.141	1.1389	1.1373	1.134	1.1343	1.1353
d	0.45	0.44	0.44	0.43	0.42	0.40	0.26	0.15	0.09
b	0.25	0.21	0.18	0.15	0.13	0.11	0.04	0.01	0.00
r	−0.27	−0.20	−0.15	−0.11	−0.08	−0.06	−0.01	0.00	0.00
% back-donation	35	32	29	26	23	21	12	5	1
				$Cr(CO)_6$					
r_{C-O}	1.1499	1.1461	1.1431	1.1406	1.1386	1.1371	1.1342	1.1346	1.1354
d	0.53	0.52	0.50	0.47	0.44	0.39	0.23	0.15	0.10
b	0.29	0.25	0.21	0.17	0.14	0.11	0.03	0.00	0.00
r	−0.27	−0.20	−0.16	−0.12	−0.10	−0.08	−0.02	−0.01	0.00
% back-donation	35	32	29	26	24	22	10	3	1
				$[Ir(CO)_6]^{3+}$					
r_{C-O}	1.1211	1.1205	1.1203	1.1203	1.1205	1.1209	1.1232	1.1253	1.1268
d	0.51	0.56	0.58	0.57	0.55	0.52	0.33	0.20	0.12
b	0.04	0.03	0.02	0.01	0.00	0.00	0.00	0.00	0.00
r	−0.20	−0.14	−0.10	−0.07	−0.06	−0.04	−0.01	0.00	0.00
% back-donation	8	5	3	2	1	0	0	0	0

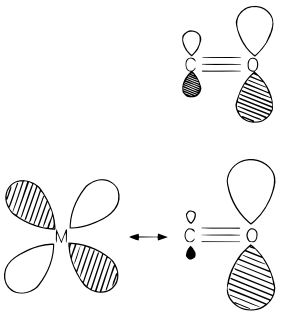

Figure 6. Schmatic representation of the influence of the repulsive polarization *r* (interaction of occupied orbitals) between the metal and CO on the polarization of the CO π-bond and, thus, on the C−O bond length.

Summary

The calculations at B3LYP/II, BP86/II, and MP2/II give accurate geometries and reliable trends for the CO stretching frequencies of the isoelectronic hexacarbonyls $[Hf(CO)_6]^{2-}$, $[Ta(CO)_6]^{-}$, $W(CO)_6$, $[Re(CO)_6]^{+}$, $[Os(CO)_6]^{2+}$, and $[Ir(CO)_6]^{3+}$. The calculated C−O bond lengths show a regular decrease from $[Hf(CO)_6]^{2-}$ to $[Ir(CO)_6]^{3+}$ at all levels of theory employed in this study. $[Ir(CO)_6]^{3+}$ has the highest bond dissociation energy for removing one carbonyl ligand. The calculated FDEs show the trend $[Ir(CO)_6]^{3+}$ > $[Os(CO)_6]^{2+}$ > $[Hf(CO)_6]^{2-}$ > $[Re(CO)_6]^{+}$ > $W(CO)_6$ ≈ $[Ta(CO)_6]^{-}$. B3LYP and BP86 give bond energies similar to those of CCSD(T) using MP2 optimized geometries. The calculated trend of the FDEs does not correlate with the C−O bond length. Analysis of the metal−CO interactions using the CDA method shows a regular decrease of metal→CO π-back-donation from $[Hf(CO)_6]^{2-}$ to $[Ir(CO)_6]^{3+}$. Optimization of the CO bond length of $[Hf(CO)_6]^{2-}$ as a function of the M−CO distance gives a smooth curve from the equilibrium value, which is longer than in free CO, to the value of free CO. $W(CO)_6$ and $Cr(CO)_6$ show a turning point in the C−O distance when one CO dissociates from the metal. The calculations of $[Ir(CO)_6]^{3+}$ show a further shortening of the CO bond length, which is shorter than in free CO, when the Ir−CO distance is stretched up to ∼0.25 Å. After this, the CO bond becomes longer and approaches the value of free CO. The CDA results indicate that the change in the C−O distances can be correlated to the M→CO π-back-donation. The M↔CO repulsive interaction has also an influence on the C−O bond distance, which seems to be the reason the C−O bond of $[Ir(CO)_6]^{3+}$ becomes at first slightly shorter when one CO dissociates.

Acknowledgment. This work was supported by the Deutsche Forschungsgemeinschaft (SFB 260 and Graduiertenkolleg Metallorganische Chemie) and the Fonds der Chemischen Industrie. R.K.S. thanks the Soros Foundation for financial support. We thank Prof. S. H. Strauss for fruitful discussions and a preprint of ref 15. Helpful discussions with U. Pidun are gratefully acknowledged. The criticism and comments of one reviewer have been very helpful in the preparation of the final version of the paper. Excellent service by the Hochschulrechenzentrum of the Philipps-Universität Marburg is gratefully acknowledged. Additional computer time was provided by the HHLRZ Darmstadt and the HLRZ Jülich.

OM970671E